Received: 26 September 2021 | Accepted: 3 January 2022

DOI: 10.1111/1759-7714.14321

ORIGINAL ARTICLE

WILEY

circFIG 4 drives the carcinogenesis and metastasis of esophagus cancer via the miR-493-5p/E2F3 axis

Zhen Huang[1†] | **Chunyue Wang**[2†] | **Xin Zhao**[2]

[1]Department of Thoracic Surgery, Zhangzhou Affiliated Hospital of Fujian Medical University, Zhangzhou, China

[2]Department of Medical Oncology, Xiamen Key Laboratory of Antitumor Drug Transformation Research, The First Affiliated Hospital of Xiamen University, School of Clinical Medicine, Fujian Medical University, Xiamen, China

Correspondence
Xin Zhao, Department of Medical Oncology, Xiamen Key Laboratory of Antitumor Drug Transformation Research, The First Affiliated Hospital of Xiamen University, School of Clinical Medicine, Fujian Medical University, No. 12 Hubin West Road, Siming District, Xiamen City, Fujian Province, China.
Email: zhaoxin2021202107@126.com

Abstract

Background: Esophageal cancer (EC) is a highly malignant tumor of the digestive tract. Circular RNAs (circRNAs) have been verified to play a regulatory role in the occurrence and progression of different cancers, including EC. This research aimed to investigate the role and molecular mechanism of circFIG 4 in EC progression.

Methods: The analyses of circFIG 4, miR-493-5p, and neuro-oncological ventral antigen 2 levels were administrated by quantitative real-time polymerase chain reaction. The characteristics of circFIG 4 were determined by Ribonuclease R assay and Actinomycin D assay. Cell proliferation was assessed via colony formation assay and 5-ethynyl-2′-deoxyuridine incorporation assay. Cell cycle distribution and apoptosis were evaluated by flow cytometry. Western blot was performed to assess protein expression. The targeted interaction among circFIG 4, miR-493-5p, and E2F transcription factor 3 (E2F3) were validated using dual-luciferase reporter or RNA immunoprecipitation assays.

Results: circFIG 4 was overtly upregulated in EC and was relatively stable in EC cells. circFIG 4 knockdown impeded proliferation, migration, and invasion and expedited apoptosis in EC cells. circFIG 4 served as a miR-493-5p sponge to act in the development of EC. Furthermore, circFIG 4 modulated EC progression via targeting miR-493-5p and miR-493-5p suppressed EC progression via targeting E2F3. circFIG 4 modulated E2F3 expression through acting as a sponge of miR-493-5p. Moreover, circFIG 4 knockdown inhibited EC tumorigenesis by targeting miR-493-5p/E2F3 axis tumor growth in vivo.

Conclusion: circFIG 4 silence mitigated EC malignant progression at least partly by mediating the miR-493-5p/E2F3 pathway, highlighting new biomarkers and therapeutic targets for EC treatment.

KEYWORDS
circFIG 4, E2F3, EC, miR-493-5p

INTRODUCTION

Esophageal cancer (EC) is a common frequently reported gastrointestinal malignancy with poor prognosis and strong aggressiveness.[1] Due to the limited treatment options for EC patients and diagnosis often at the advanced stage of cancer, the overall survival rate remains unsatisfactory.[2,3] Therefore, it is crucial to elucidate the pathogenesis of EC and find novel useful diagnostic markers for EC therapy.

Circular RNAs (circRNAs) are a sort of noncoding RNA possessing covalent closed loops by a covalent linkage at the 3′ and 5′ ends.[4–6] In recent years, diverse circRNAs have been illuminated to be abnormally expressed in tumors and linked to the pathogenesis of human cancers by interacting with microRNAs (miRNAs),[7] including EC.[8] For example, circ-PRMT5 promoted the metastasis of EC by binding to miR-203.[9] circFIG 4 (also termed as hsa_circ_0077607), derived from FIG 4 precursor mRNA, was located at chr6: 110036280–110 064 975. Previous study uncovered that circFIG 4 was abundantly expressed

[†]These authors contributed equally to this work.

in EC tissues.[10,11] Nonetheless, the potential biological function of circFIG 4 in the pathogenesis of EC has not been clarified.

miRNAs are characterized by being ~22 nucleotides in length and directly modulate the expression of genes via recognition of the 3′UTR of targeted messenger RNAs (mRNAs).[12–14] The dysregulation of miRNAs has been confirmed to exert a key role in the modulation of tumor biological processes of multiple cancers,[15] including EC.[16] Bian et al. reported that miR-493 had reduced expression in EC, and its overexpression inhibited EC development.[17] In this report, it was unveiled that miR-493-5p was strikingly lower We have made revisions as suggested. expressed in EC. However, the interplay between circFIG 4 and miR-493-5p has not yet been identified.

We verified the low expression of circFIG 4 in EC. Mechanically, the target miRNAs of circFIG 4 and related pathways in EC pathogenesis were explored. These findings might provide new therapeutic biomarkers and targets for EC diagnosis or therapy.

MATERIALS AND METHODS

Tissue samples

Fifty-four paired EC tissues and neighboring healthy tissues were gathered from 54 EC patients after surgery at Zhangzhou Affiliated Hospital of Fujian Medical University. These participants signed informed consent and this research was ratified by the Ethical Committee of Zhangzhou Affiliated Hospital of Fujian Medical University.

Cell culture

Normal esophageal epithelial cells (HET-1A) were acquired from the American Type Culture Collection (ATCC, Manassas, VA). EC cell lines (KYSE-410, KYSE-150, Eca-109, and EC9706) were commercially obtained from Tongpai Biological Technology Co., Ltd. All cells were fostered in RPMI-1640 medium (Solarbio) plus 10% fetal bovine serum (FBS, Solarbio) and 1% penicillin–streptomycin (Procell) in a humidified CO_2 (5%) incubator at 37°C.

Quantitative real-time polymerase chain reaction

Triquick Reagent (Solarbio) was applied for RNA segregation. The inverted transcription was conducted using a PrimerScript RT Reagent kit (Takara) or a PrimeScript miRNA RT-PCR Kit (Takara). Subsequently, a SYBR Premix Ex Taq II kit (Takara) was employed for quantitative real-time polymerase chain reaction (qRT-PCR) assay on a PCR system. The primers exhibited in Table 1 were used for PCR amplification. β-actin and U6 were chosen as the inner contrasts, and the relative RNA expression was computed via the $2^{-\Delta\Delta Ct}$ strategy.

TABLE 1 Primer sequences used for qRT-PCR

Name		Primers for PCR (5′–3′)
circFIG4	Forward	ATGTGGCTGCCCTTCACTTT
	Reverse	CGTTTCTGCATTATTGCTCCCA
FIG4	Forward	CCATCATCAGCTCGGTCCAG
	Reverse	AAGATCCAAGCGGCCAAGAA
miR-374a-5p	Forward	GCCGAGTTATAATACAACC
	Reverse	CTCAACTGGTGTCGTGGAG
miR-374b-5p	Forward	GCCGAGATATAATACAACC
	Reverse	CTCAACTGGTGTCGTGGAG
miR-493-5p	Forward	GCCGAGTTGTACATGGTAGG
	Reverse	CTCAACTGGTGTCGTGGAG
miR-520g-3p	Forward	GCCGAGACAAAGTGCTTCC
	Reverse	CTCAACTGGTGTCGTGGAG
miR-520h	Forward	GCCGAGACAAAGTGCTTCC
	Reverse	CTCAACTGGTGTCGTGGAG
E2F3	Forward	TGCACTACGAAGTCCAGATAGTC
	Reverse	GCACTTCTGCTGCCTTGTTC
β-actin	Forward	CTTCGCGGGCGACGAT
	Reverse	CCACATAGGAATCCTTCTGACC
U6	Forward	CTCGCTTCGGCAGCACA
	Reverse	AACGCTTCACGAATTTGCGT

Ribonuclease R and Actinomycin D assays

For the ribonuclease R (RNase R) assay, 4 μg of isolated RNA was kept with RNase R (3 U/μg; Solarbio) or not for 30 min at 37°C. For the Actinomycin D assay, KYSE410 and ECA109 cells were stimulated with 2 μg/mL Actinomycin D (Solarbio) for 0, 6, 12, 18, and 24 h. The relative RNA abundances of circFIG 4 and linear FIG 4 mRNA were assessed by qRT-PCR analysis.

Cell transfection

Short hairpin RNA against circFIG 4 (sh-circFIG 4) was established to silence circFIG 4, with sh-NC as matched contrast. For miR-493-5p overexpression or inhibition, miR-493-5p mimic or inhibitor (miR-493-5p or in-miR-493-5p) was constructed, with miR-NC or in-miR-NC as control. The E2F3 overexpression vector (E2F3) was constructed through introducing the sequence of E2F3 into the pcDNA3.1 (pcDNA) vector, with empty pcDNA vector as a control. All these designated oligonucleotides and vectors were synthesized by GenePharma and individually transduced into KYSE-150 and Eca-109 cells through Lipofectamine 3000 (Invitrogen).

Colony formation assay

Two hundred transfected KYSE-150 and Eca-109 cells were planted into 24-well plates and trained at 37°C for 14 days. After fixing with paraformaldehyde (4%; Beyotime) and staining with crystal violet (0.5%; Beyotime), the colonies (> 50 cells) were observed and counted using a microscope for at least three independent replications.

EdU incorporation assay

A 5-ethynyl-2′-deoxyuridine (EdU) staining proliferation kit (Abcam) was employed for the determination of DNA synthetic capacity in proliferating cells. In general, transduced KYSE-150 and Eca-109 cells were planted in 96-well plates at 37°C for 48 h. Subsequently, to each well was added 50 μM EdU for 2 h of incubation. Then, cells were subjected to fixation with 4% paraformaldehyde (Beyotime) for 20 min. Later, cells were further incubated with Apollo reaction cocktail and Hoechst 33342 (Abcam) for 30 min in darkness for nuclear counterstain. Finally, an inverted microscope (100×) was applied to calculate the number of EdU-positive cells (cyan cells) in five randomly selective areas.

Flow cytometry assay

Flow cytometry was used for the detection of cell cycle distribution and cell apoptosis. After being transfected for 48 h, KYSE-150 and Eca-109 cells were harvested. For the determination of cell cycle distribution, transduced KYSE-150 and Eca-109 cells were gathered and washed with phosphate buffer solution (PBS), followed by immobilization with 70% ethanol at 4°C overnight. Then the cells were resuspended in binding buffer and dyed with propidine iodide (PI; Solarbio) in the dark at 37°C for 30 min. Finally, the distributed proportions of KYSE-150 and Eca-109 cells at different phases (G0/G1, S, and G2) were monitored through a flow cytometer.

An Annexin V-FITC/PI Apoptosis Detection kit (Solarbio) was utilized for apoptotic detection. Briefly, transfected KYSE-150 and Eca-109 cells were dyed using Annexin V-FITC and propidium iodide (PI) in darkness for 15 min. The apoptotic rate of KYSE-150 and Eca-109 cells (Annexin V-FITC$^+$ and PI$^+$ or PI$^-$) was measured using a flow cytometer.

Western blot

Protein was extractive via RIPA buffer (Solarbio) and segregated by 10% SDS-PAGE gel (Beyotime), then transferred onto PVDF membrane (Millipore). After sealing with 5% skimmed milk for 1 h in an indoor environment, the membrane was probed with primary antibodies against Bcl-2-associated X protein (Bax, 1:2000, ab263897; Abcam), B-cell lymphoma/leukemia-2 (Bcl-2, 1:2000, ab196495; Abcam), E2F3 (1:2000, ab152126; Abcam), and internal protein standard β-actin (1:200, ab115777; Abcam) at 4°C for 24 h. Next, the membrane was incubated with secondary antibody (1:25000, ab205718; Abcam) for 2 h. Subsequently, the immunoblots were visualized using a BeyoECL Star Kit (Beyotime).

Wound healing assay

The migratory capacity of KYSE-150 and Eca-109 cells was tested through conducting a wound healing assay. Transfected cells were planted in 24-well plates for 24 h, and subsequently cell monolayers were gently scratched using 200-μL sterilized pipette tips and rinsed using PBS for the removal of detached cells, followed by the cultivation for an additional 24 h in medium without serum. The widths of wounds were photographed with an optical microscope (40×) at 0 and 24 h.

Transwell invasion assay

For the detection for invasion, a transwell assay was implemented utilizing a 24-well transwell chamber (8 μm; BD Biosciences) covered with matrigel (BD Biosciences). Transfected cells in medium without serum were planted in the top chamber, while medium with FBS was placed in the bottom chamber. Twenty-four hours later, the invaded cells were treated using paraformaldehyde (4%; Beyotime) and crystal violet (Beyotime) for 1 h, and then photographed and counted under a microscope (100×) from five randomly chosen regions.

Dual-luciferase reporter assay

The fragments of circFIG 4 or E2F3 3′UTR possessing the presumptive or mutant target sites of miR-493-5p were severally introduced into pmirGLO vector (Promega), forming wild-type circFIG 4 or E2F3 (circFIG 4 WT or E2F3 3′UTR WT) and mutant-type circFIG 4 or E2F3 (circFIG 4 MUT or E2F3 3′UTR MUT) luciferase reporter vectors. Subsequently, the constructed reporter vectors and miR-NC or miR-493-5p were transfected into EC cells. Forty-eight hours later, the luciferase intensity was tested via a Dual-Lucy Assay Kit (Solarbio).

RNA immunoprecipitation assay

EC cells were gathered and an RNA immunoprecipitation (RIP) assay was executed using an EZ-Magna RIP Kit (Millipore). Briefly, cell lysates acquired through dissociation using RIP lysis buffer were reacted with magnetic beads conjugated with Anti-Ago2 and Anti-IgG for 8 h at 4°C. Finally, the RNAs remaining on the beads were isolated

from the complexes, then subjected to qRT-PCR assay to detect the abundances of circFIG 4 and miR-493-5p.

Xenograft tumor model

Ten male BALB/c nude mice (about 5 weeks old) were obtained from Beijing Vital River Laboratory Animal Technology Co., Ltd. The mice were arbitrarily grouped into two groups (n = 5/group) at random: sh-NC or sh-circFIG 4. KYSE-150 cells in 200 μL of PBS (Solarbio) stably introduced with sh-NC or sh-circFIG 4 were inoculated into the mice through subcutaneous injection. Tumor volume was monitored weekly via the formula: 0.5 × length × width^2. At day 35, all mice were sacrificed and the excised transplanted neoplasms were weighed. The protocols of the animal study were empowered by the Animal Care and Use Committee of Zhangzhou Affiliated Hospital of Fujian Medical University.

Immunohistochemistry assay

The paraffin-embedded tissue sections derived from transplanted neoplasms in the sh-NC or sh-circFIG 4 groups

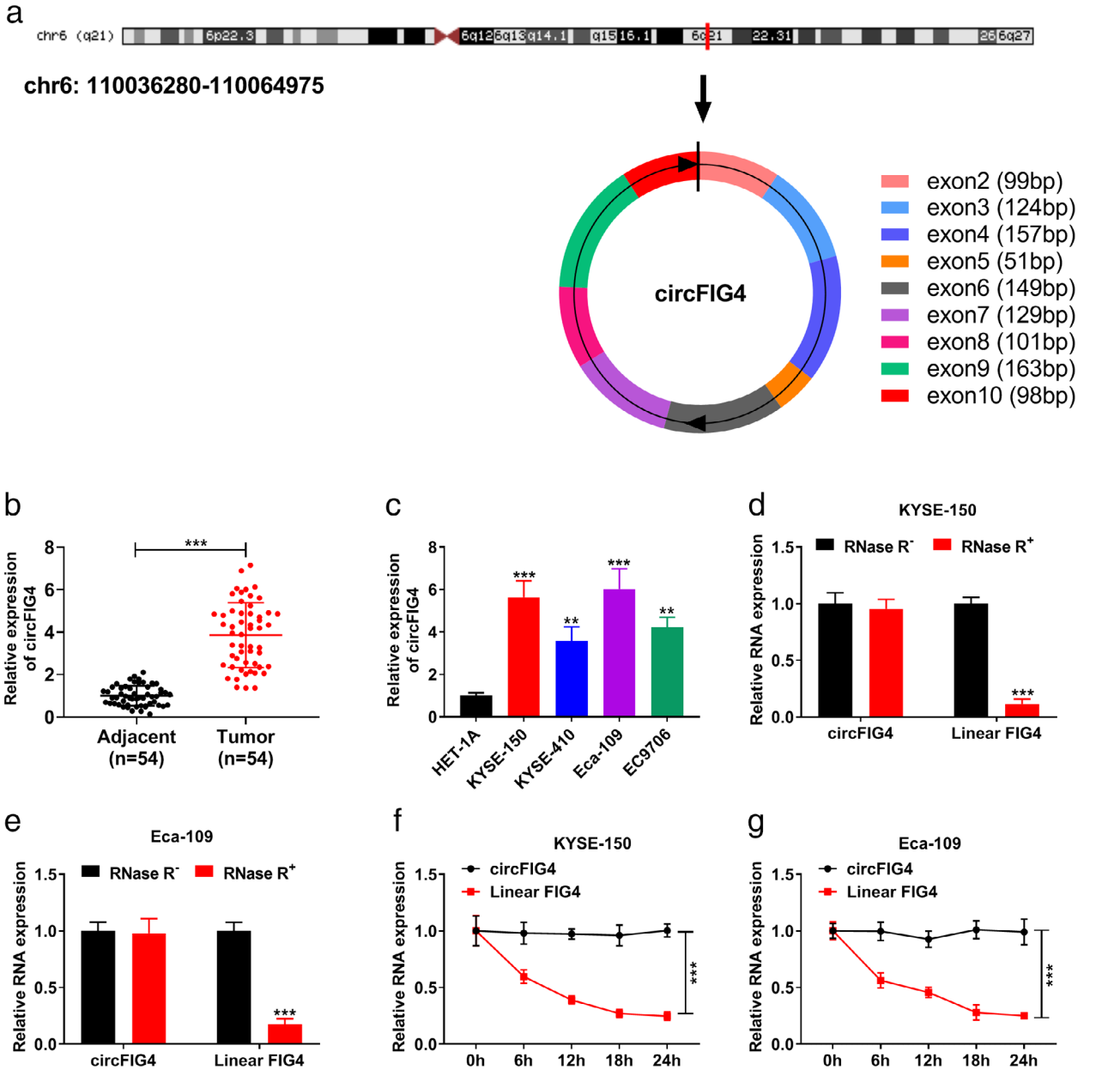

FIGURE 1 circFIG 4 was upregulated in EC tissues and cells. (A) Schematic diagram of circFIG 4 biogenesis via a back-splicing mechanism. (B) The expression of circFIG 4 in EC tissues (Tumor, n = 54) and adjacent normal tissues (Adjacent, n = 54) was determined by qRT-PCR. (C) The expression of circFIG 4 in EC cell lines (KYSE-150, KYSE-410, Eca-109, and EC9706) and normal HET-1A was measured using qRT-PCR. (D and E) circFIG 4 and linear FIG 4 levels were tested by qRT-PCR in KYSE-150 and Eca-109 cells following RNase R digestion. (F and G) The levels of circFIG 4 and linear FIG 4 were detected by qRT-PCR in KYSE-150 and Eca-109 cells after Actinomycin D stimulation. $^{**}p < 0.01$, $^{***}p < 0.001$

(n = 5/group) were dewaxed and sectioned (4 μm). Afterwards, the tissue sections were co-reacted with primary antibodies against ki-67 (1:200, ab16667; Abcam) overnight at 4°C, and then reacted with secondary antibody (1:2000, ab205718; Abcam) in an indoor environment for 1 h. Next, 3,3′-diaminobenzidine solution (DAB; Beyotime) was

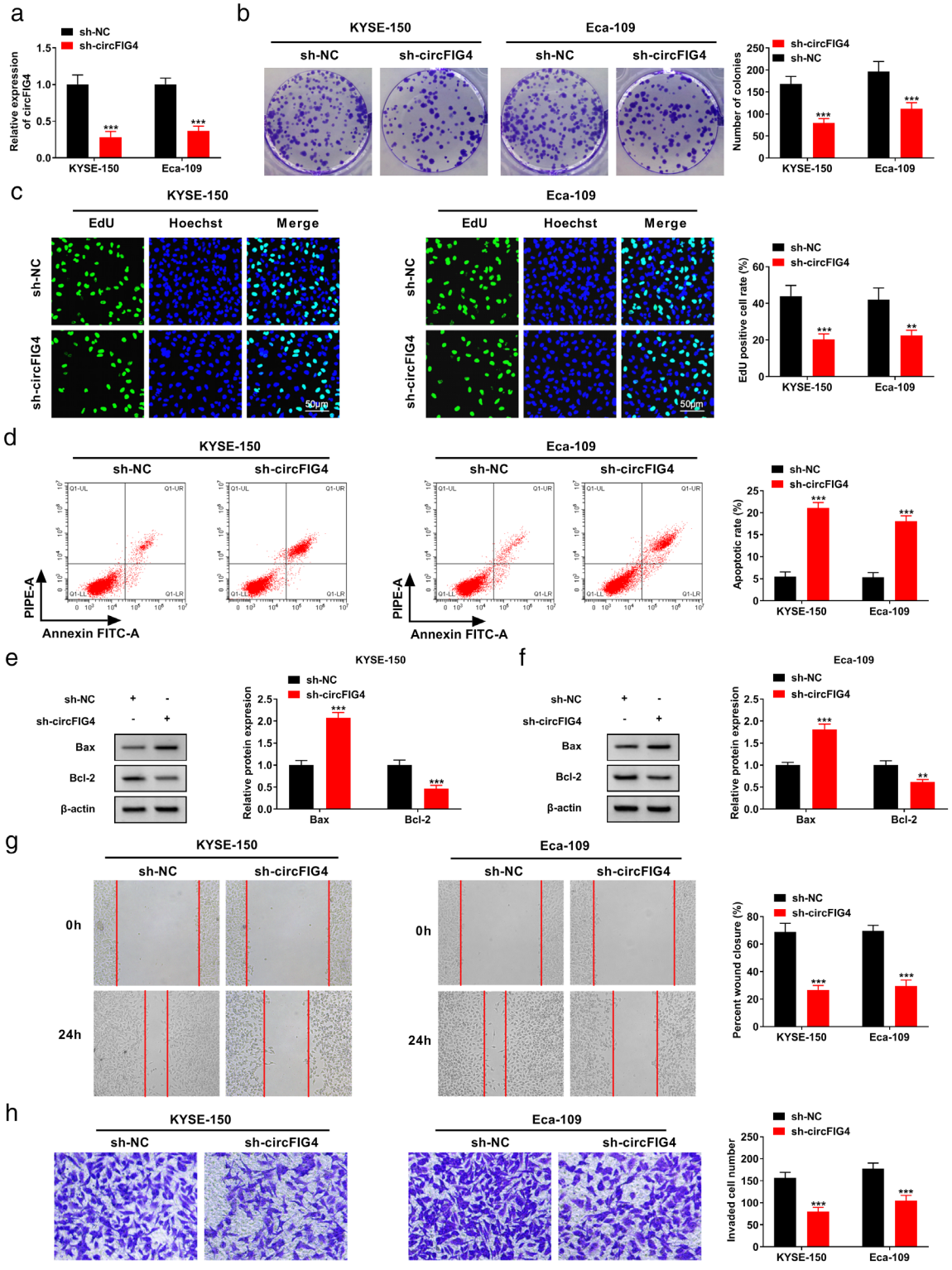

FIGURE 2 Downregulated circFIG 4 inhibited EC cell proliferation and metastasis, and induced cell apoptosis. KYSE-150 and Eca-109 cells were introduced with sh-NC or sh-circFIG 4. (A) The knockdown efficiency of circFIG 4 was detected using qRT-PCR. (B and C) Cell proliferation assessment was completed via colony formation assay (B) and EdU incorporation assay (C). (D) The apoptotic rate was evaluated by flow cytometry. (E and F) Western blot was applied to detect the protein levels of Bax and Bcl-2. (G) Cell migration capacity was monitored by wound healing assay. (H) Cell invasion was tested using a transwell assay (100×). $^{**}p < 0.01$, $^{***}p < 0.001$

utilized for 10 min dyeing of tissue slices and hematoxylin (Beyotime) was employed for the counterstain of nuclei. The representational images were acquired using a fluorescence microscope with appropriate magnification.

To assess the degree of positive staining for ki-67 antibody in tumor cells, the immunoreactivity score (IRS) was evaluated by referring to previous report of Striefler et al.[18] in which the final total score was generated by the multiplication product of the intensity score (the staining intensity) and the proportion score (the percentage of positive cells). The intensity score was defined as follows: negative = 0 (no staining), weak staining = 1, moderate staining = 2, strong staining = 3. The proportion score was defined as follows: 0% = 0 (no stained cells in any field), 1–10% of the nuclear staining-positive cells = 1, 11–50% stain-positive cells = 2, 51–80% stain-positive cells = 3, 81–100% stain-positive cells = 4. The total IRS score ranged from 0 to 12. IRS was determined by two different observers, and the observers were blinded for the specimen data during the scoring procedures. The median values of the three observations were used as the final scores. The distribution of staining in the sh-circFIG 4 group ($n = 5$) was compared with that in the sh-NC group ($n = 5$).

Statistical analysis

All data from at least three replicates were displayed as mean ± standard deviation (SD). Statistical analyses for data were conducted by SPSS 24.0 software. The differences were assessed by Student's *t*-test or one-way analysis of variance. The linear relations among circFIG 4, miR-493-5p, and E2F3 levels in EC tissues were confirmed via Spearman's correlation coefficient analysis. $p < 0.05$ indicated statistical significance.

RESULTS

circFIG 4 was highly expressed in EC tissues and cells

circFIG 4 (circ_0086720) was located in chr6: 110036280–110 064 975 and derived from exon 2–10 of the FIG 4 gene via the back-splicing mechanism (Figure 1A). And the generation process of circFIG 4 was shown in Figure 1A. The expression of circFIG 4 in EC tissues and cells was determined. The results of the qRT-PCR assay show that the circFIG 4 level was remarkably increased in EC tissues (Tumor, $n = 54$)

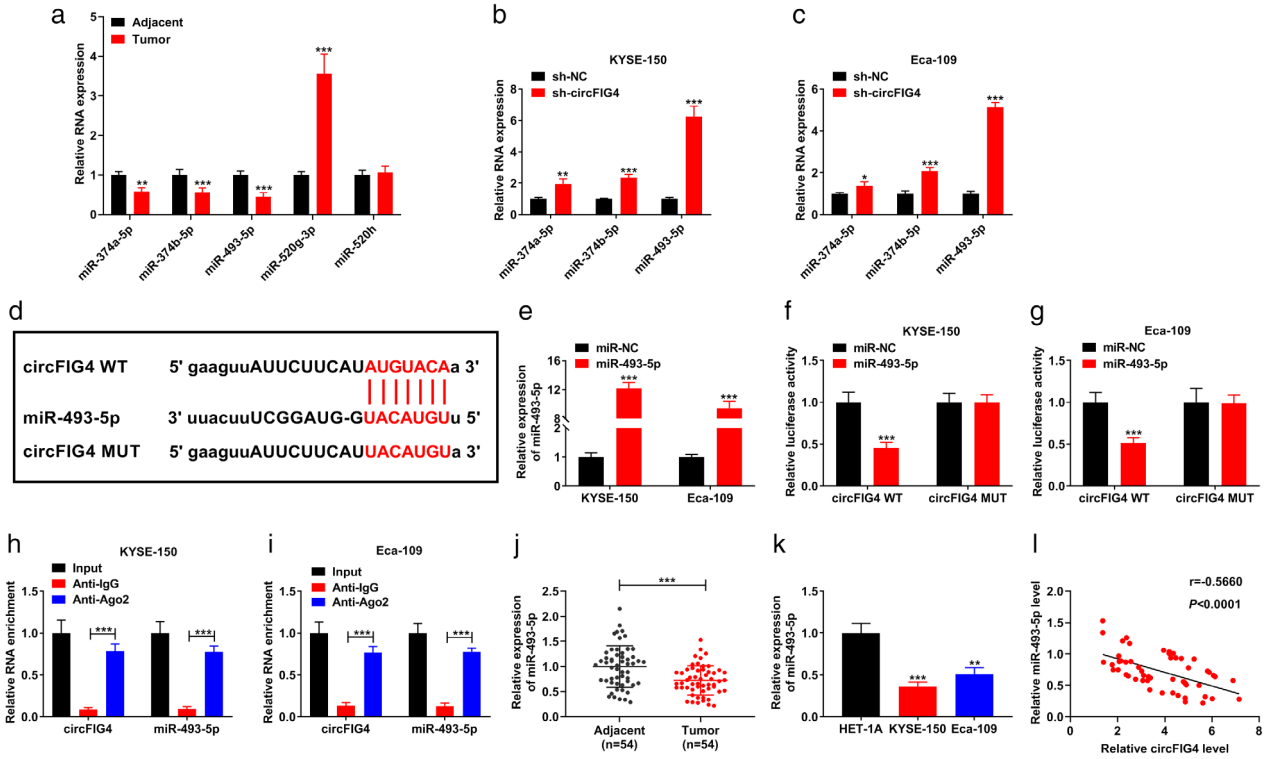

FIGURE 3 circFIG 4 sequestered miR-493-5p in EC cells. (A) The expression of five miRNAs that had a targeted binding sequence with circFIG 4 in EC tissues and adjacent normal tissues was monitored by qRT-PCR. (B and C) The expression of miR-374a-5p, miR-374b-5p, and miR-493-5p in KYSE-150 and Eca-109 cells after circFIG 4 knockdown was detected by qRT-PCR. (D) The binding sites between circFIG 4 and miR-493-5p. (E) The expression of miR-493-5p in KYSE-150 and Eca-109 cells after miR-493-5p or miR-NC transfection. (F and G) Luciferase activity was detected in KYSE-150 and Eca-109 cells co-transfected with circFIG 4 WT or circFIG 4 MUT and miR-NC or miR-493-5p. (H and I) Cellular lysates of KYSE-150 and Eca-109 cells were incubated with anti-Ago2 or anti-IgG antibody, and then circFIG 4 and miR-493-5p levels were detected by qRT-PCR. (J) The expression of miR-493-5p in EC tissues (Tumor, $n = 54$) compared to adjacent normal tissues (Adjacent, $n = 54$) was examined by qRT-PCR. (K) The expression of miR-493-5p in EC cell lines (KYSE-150 and Eca-109) and normal HET-1A was checked using qRT-PCR. (L) The linear relation between circFIG 4 and miR-493-5p expression in EC tissues was analyzed using Spearman's correlation coefficient analysis. $^{*}p < 0.05$, $^{**}p < 0.01$, $^{***}p < 0.001$

compared to adjacent normal tissues (Adjacent, $n = 54$) (Figure 1B). Meanwhile, high expression of circFIG 4 was also observed in EC cell lines (KYSE-150, KYSE-410, Eca-109, and EC9706) relative to that in the normal HET-1A cell line (Figure 1C). To identify the stability of circFIG 4, RNase R and Actinomycin D treatments were performed. RNase R digestion assay manifested that circFIG 4 was resistant to RNase R treatment in KYSE-150 and Eca-109 cells compared to linear FIG 4 mRNA (Figure 1D,E). The Actinomycin D assay showed that the half-life of circFIG 4 was longer than that of linear FIG 4 in KYSE-150 and Eca-109 cells (Figure 1F, G). These data demonstrate that circFIG 4 was upregulated in EC with stable structure.

circFIG 4 depletion blocked proliferation and metastasis, and induced apoptosis in EC cells

To elucidate the function of circFIG 4 in EC development, a series of loss-of-function tests was performed via transfecting sh-NC or sh-circFIG 4 into KYSE-150 and Eca-109 cells. As shown in Figure 2A, the reduced expression of circFIG 4 in KYSE-150 and Eca-109 cells after sh-circFIG 4 introduction proved the high silencing efficiency of circFIG 4. As demonstrated by colony formation assay and EdU assay, deficiency of circFIG 4 remarkably reduced the colony number and EdU positive cell rate of KYSE-150 and Eca-109 cells (Figure 2B,C), implying that cell proliferation was impeded by circFIG 4 downregulation. Meanwhile, the percentages of KYSE-150 and Eca-109 cells (%) at the G0/G1 stage were evidently increased by the downregulation of circFIG 4 through flow cytometry analysis, suggesting that circFIG 4 silence promoted cell cycle arrest (Supporting Information Figure S1A,B). Flow cytometry also showed that circFIG 4 knockdown strikingly increased the apoptotic rate of KYSE-150 and Eca-109 cells (Figure 2D). Besides, the level of pro-apoptosis protein Bax was increased while the level of anti-apoptosis protein Bcl-2 was decreased in KYSE-150 and Eca-109 cells after circFIG 4 depletion (Figure 2E,

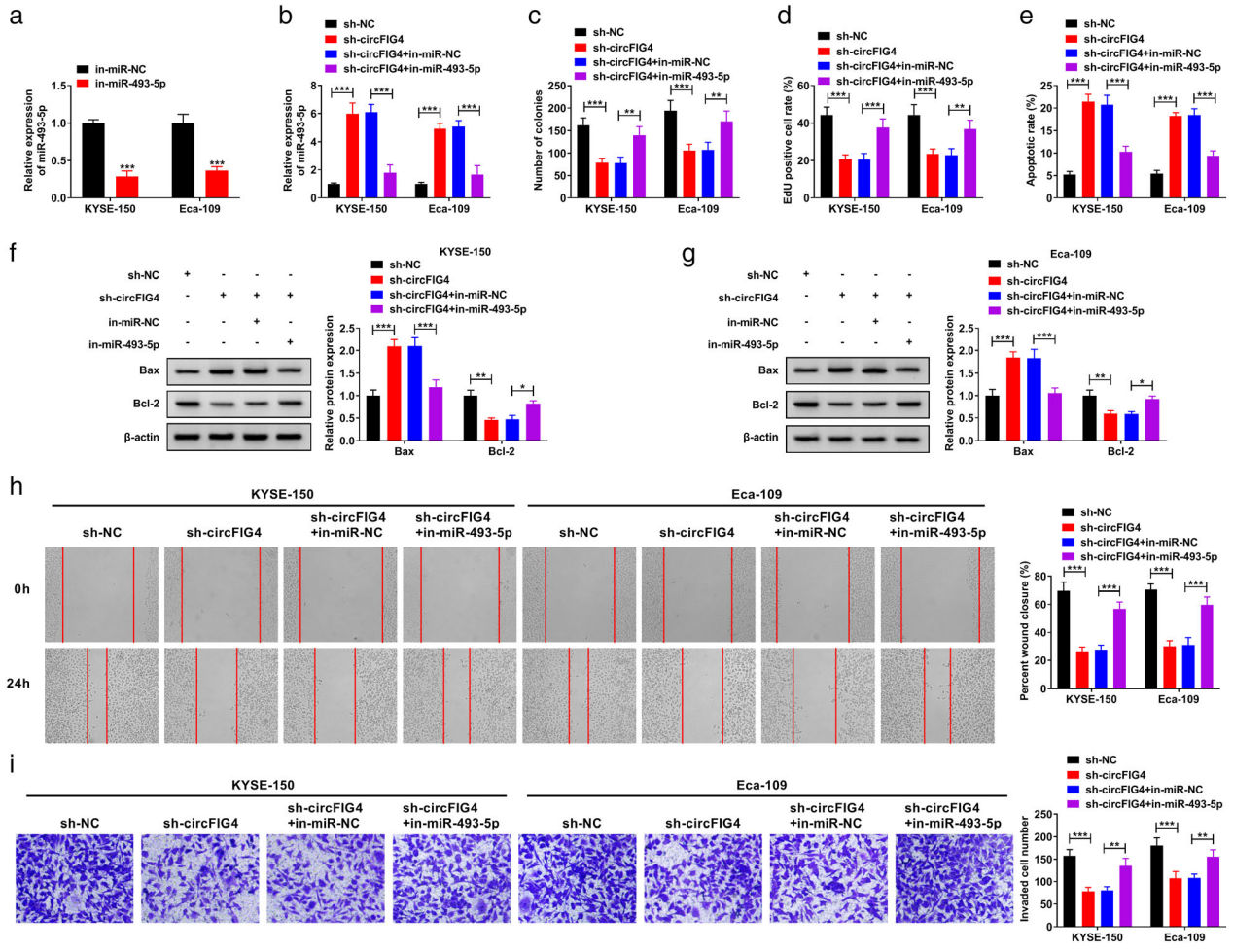

FIGURE 4 Silence of circFIG 4 inhibited EC cell malignant behaviors by modulating miR-493-5p. (A) The qRT-PCR was exploited to evaluate the knockdown efficiency of in-miR-493-5p in KYSE-150 and Eca-109 cells. (B–I) KYSE-150 and Eca-109 cells were transfected with sh-NC, sh-circFIG 4, sh-circFIG 4 + in-miR-NC or sh-circFIG 4+in-miR-493-5p, followed by determination of the miR-493-5p level by qRT-PCR (B), the number of colonies by clone formation assay (C), cell proliferation by EdU incorporation assay (D), cell apoptosis by flow cytometry (E), levels of Bax and Bcl-2 by western blot (F and G), cell migration by wound healing assay (H), and cell invasion by transwell assay (I). $^{*}p < 0.05$, $^{**}p < 0.01$, $^{***}p < 0.001$

F). In addition, the wound healing assay and the transwell invasion assay showed that circFIG 4 knockdown visibly suppressed the migration and invasion of KYSE-150 and Eca-109 cells, respectively (Figure 2G,H). These results demonstrate that knockdown of circFIG 4 repressed the malignant phenotypes of EC cells, hinting at a tumor-promoting role of circFIG 4 in EC.

circFIG 4 directly targeted miR-493-5p

To further explore the underlying basis of circFIG 4 in EC cells, the potential downstream miRNA targets of it were predicted by online software starBase (http://starbase.sysu.edu.cn/). The prediction result suggested that five miRNAs had a targeted binding sequence with circFIG 4. Through detecting the expression of the five targeted miRNA candidates in six paired randomly selected EC tissues and adjacent normal tissues, the expressions of miR-374a-5p, miR-374b-5p, and miR-493-5p were dramatically downregulated in EC tissues (Figure 3A). The expression of these three downregulated miRNAs in KYSE-150 and Eca-109 cells after circFIG 4 knockdown was monitored. The results showed that the expression of miR-493-5p was the most upregulated in KYSE-150 and Eca-109 cells after sh-circFIG 4 introduction compared with the sh-NC group (Figure 3B, C). Therefore, miR-493-5p was selected as the target of circFIG 4 in our study for subsequent experiments. The putative complementary binding sites between circFIG 4 and miR-493-5p are shown in Figure 3D. The introduction of miR-493-5p notably reinforced the expression of miR-493-5p compared to miR-NC (Figure 3E), and miR-493-5p reintroduction significantly diminished the luciferase activity in KYSE-150 and Eca-109 cells transfected with circFIG 4 WT but not circFIG 4 MUT compared with miR-NC introduction (Figure 3F,G). In addition, RIP assay indicated that circFIG 4 and miR-493-5p were abundantly captured by Ago2 antibody relative to IgG antibody in KYSE-150 and Eca-109 cells (Figure 3H,I), suggesting the endogenous interaction between circFIG 4 and miR-493-5p. Moreover, miR-493-5p expression was notably decreased in EC tissues and cells (KYSE-150 and Eca-109) compared to normal tissues and HET-1A cells (Figure 3J,K). Spearman's correlation coefficient analysis showed that there was an inverse correlation between circFIG 4 and miR-493-5p expression in EC tissues ($p < 0.0001$, $r = -0.5660$) (Figure 3L). Altogether, these outcomes demonstrated that circFIG 4 might serve as a molecular sponge for miR-493-5p.

Silence of circFIG 4 decelerated EC cell malignant behaviors by modulating miR-493-5p

Based on the targeting relationship between circFIG 4 and miR-493-5p, whether or not the function of circFIG 4 in EC progression was associated with its sponge effect on miR-493-5p was investigated. KYSE-150 and Eca-109 cells were transfected with miR-493-5p inhibitor (in-miR-493-5p) to silence its expression (Figure 4A). The functional experiments were performed in KYSE-150 and Eca-109 cells introduced with sh-circFIG 4, sh-circFIG 4+in-miR-493-5p or the matched control groups. As expected, the introduction of in-miR-493-5p partially relieved the increase in miR-493-5p level caused by circFIG 4 silence (Figure 4B). Subsequent experiments results showed that the inhibitory effects of circFIG 4 silencing on cell colony formation (Figure 4C),

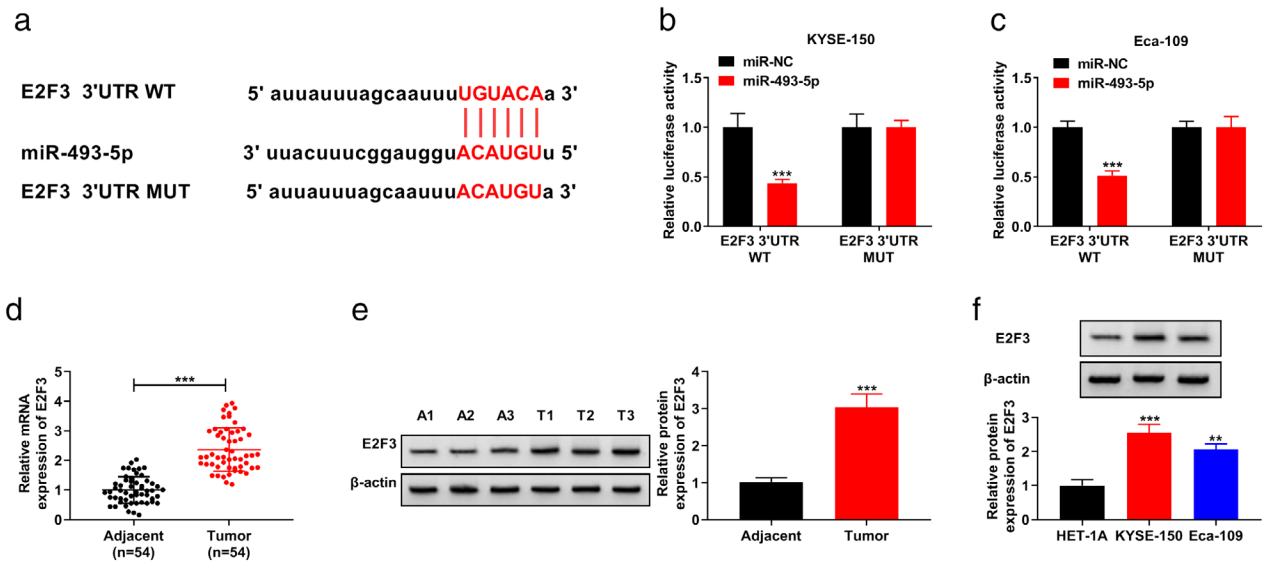

FIGURE 5 E2F3 was a target of miR-493-5p. (A) The putative binding sequence between miR-493-5p and E2F3 3′UTR was exhibited. (B and C) Relative luciferase activity in the cells co-transfected with E2F3 3′UTR WT or E2F3 3′UTR MUT and miR-NC or miR-493-5p. (D and E) E2F3 mRNA and protein levels were detected in EC tissues (Tumor, $n = 54$) compared to adjacent normal tissues (Adjacent, $n = 54$) using qRT-PCR and western blot. (F) The protein expression of E2F3 in EC cell lines (KYSE-150 and Eca-109) and normal HET-1A was examined using western blot. $^{**}p < 0.01$, $^{***}p < 0.001$

cell proliferation (Figure 4D), the expression of Bcl-2 (Figure 4F,G), migration (Figure 4H), and invasion (Figure 4I) and stimulative effects on G0/G1 phase arrest (Supporting Information Figure S1C,D), the expression of Bax (Figure 4F,G), and cell apoptosis (Figure 4E) were remarkably alleviated by the stored expression of miR-493-5p in KYSE-150 and Eca-109 cells. All these data evidenced that circFIG 4 depletion suppressed EC development partially through regulating miR-493-5p.

E2F3 was a target of miR-493-5p

Subsequently, we further explored the underlying mechanism of circFIG 4/miR-493-5p in regulating EC development. StarBase prediction manifested that E2F3 was a target gene of miR-493-5p and the potential binding sequence is presented in Figure 5A. Transfection of miR-493-5p mimic led to a remarkable reduction in luciferase activity of the E2F3 3′UTR WT reporter, and this effect was almost completely abrogated by the site-directed mutation (Figure 5B,C). E2F3 was an aberrantly upregulated molecule in EC tissues as the qRT-PCR and western blot results in Figure 5D,E show. Also, the E2F3 level was prominently elevated in KYSE-150 and Eca-109 cells compared with THLE-2 cells (Figure 5F). These analyses explain the target relation of miR-493-5p for E2F3.

MiR-493-5p functioned as a tumor-inhibitory molecule in EC progression via targeting E2F3

To evaluate whether or not miR-493-5p regulates EC development via binding to E2F3, rescue experiments were carried out in KYSE-150 and Eca-109 cells introduced with miR-NC, miR-493-5p, miR-493-5p+pcDNA or miR-493-5p+E2F3. First, the E2F3 protein level was shown to be enhanced in KYSE-150 and Eca-109 cells after E2F3

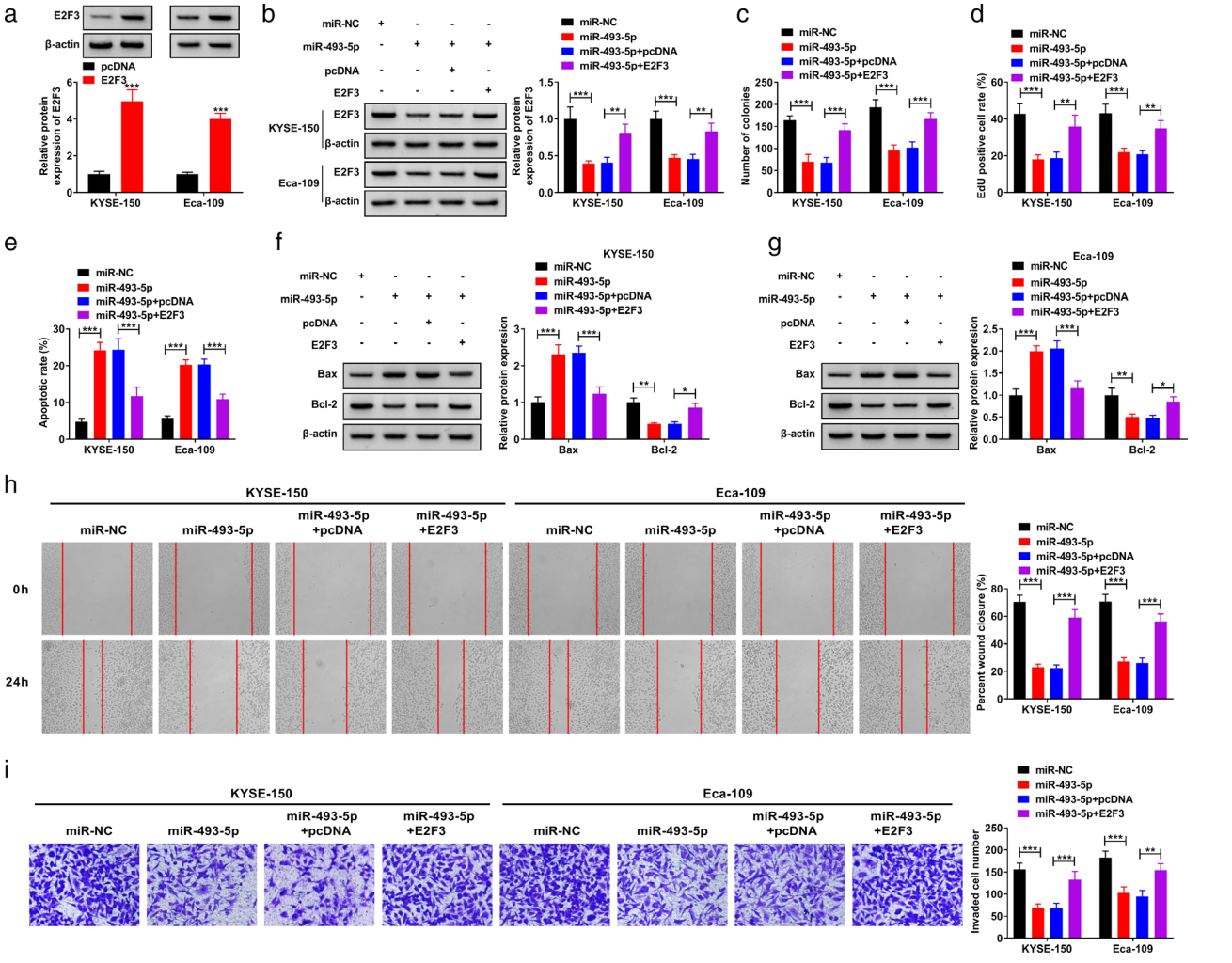

FIGURE 6 MiR-493-5p inhibited EC progression via targeting E2F3. (A) The overexpression efficiency of E2F3 in KYSE-150 and Eca-109 cells after E2F3 transfection was confirmed by western blot. (B–I) KYSE-150 and Eca-109 cells were transfected with miR-NC, miR-493-5p, miR-493-5p+pcDNA or miR-493-5p+E2F3. E2F3 protein level (B), the number of colonies (C), cell proliferation (D), apoptotic rate (E), protein levels of Bax and Bcl-2 (F and G), cell migration (H), and invasion (I) were examined by appropriate methods in transfected KYSE-150 and Eca-109 cells. $^{*}p < 0.05$, $^{**}p < 0.01$, $^{***}p < 0.001$

transfection, verifying the overexpression efficiency of E2F3 (Figure 6A). Then, E2F3 overexpression partially alleviated miR-493-5p-mediated E2F3 downregulation (Figure 6B). Furthermore, miR-493-5p upregulation significantly reduced the number of colonies (Figure 6C), cell proliferation (Figure 6D), and cycle progress (Supporting Information Figure S1E,F), and enhanced the apoptotic rate (Figure 6E), while these impacts were rescued via overexpressing E2F3. The data western blot revealed that E2F3 depletion led to an obvious suppression in Bax expression and a significant repression in Bcl-2 expression (Figure 6F,G). In addition, introduction of miR-493-5p suppressed cell migration (Figure 6H) and invasion (Figure 6I), whereas these effects were abrogated after transfection with E2F3. Collectively, these results affirmed that miR-493-5p worked as an inhibitor in EC development by downregulating E2F3.

circFIG 4 modulated E2F3 expression through binding to miR-493-5p

To further explore the relationships among circFIG 4, miR-493-5p, and E2F3, the expression of E2F3 in EC cells after transfection with sh-circFIG 4, sh-circFIG 4 + in-miR-493-5p or the matched controls was examined. The results showed that knockdown of circFIG 4 drastically repressed the protein expression of E2F3 in KYSE410 and ECA109

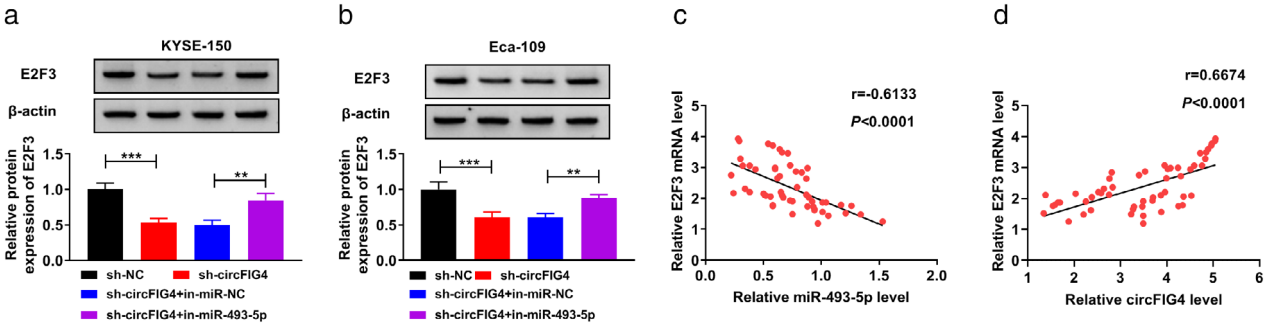

FIGURE 7 circFIG 4 acted as a miR-493-5p sponge to regulate E2F3 expression. (A and B) Western blot was carried out to examine the protein expression of E2F3 in KYSE410 and ECA109 cells introduced with sh-NC, sh-circFIG 4, sh-circFIG 4 + in-miR-NC or sh-circFIG 4 + in-miR-493-5p. (C and D) Spearman's correlation coefficient was used to analyze the correlation between E2F3 and miR-493-5p or circFIG 4. $^{**}p < 0.01$, $^{***}p < 0.001$

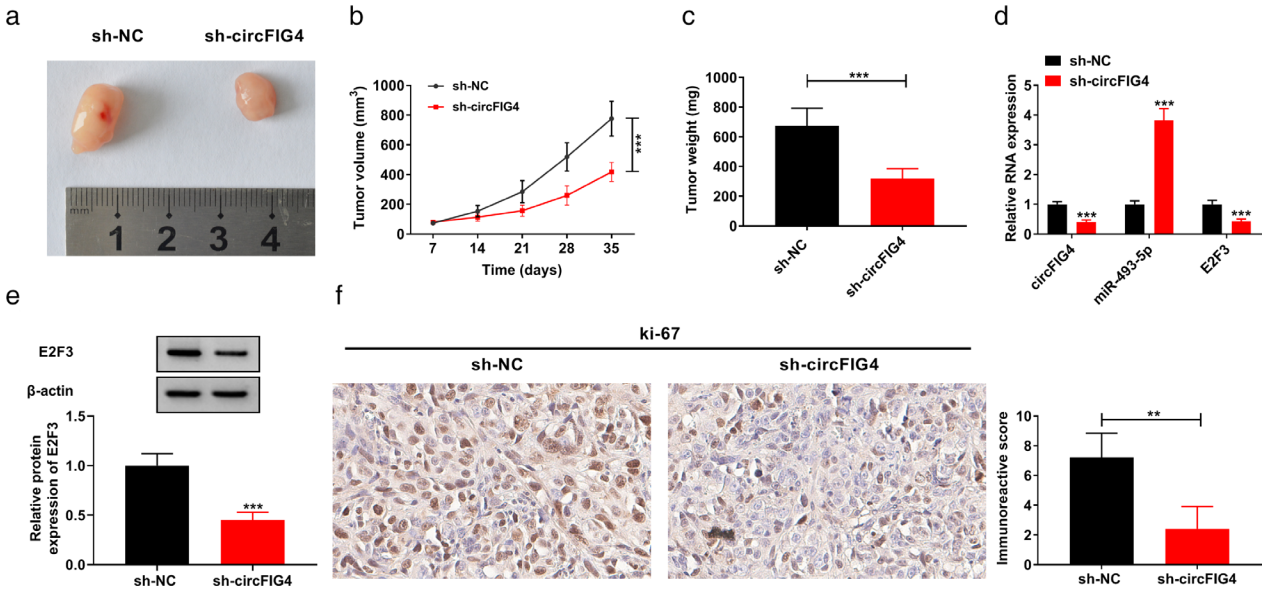

FIGURE 8 Knockdown of circFIG 4 retarded tumor growth of EC in vivo. KYSE-150 cells transfected with sh-NC or sh-circFIG 4 were subcutaneously injected into the nude mice ($n = 5$ each group). Thirty-five days later, all mice were sacrificed and tumor tissues were excised. (A) Images of solid tumors from the mice. (B) Tumor volume was measured every 7 days after 7 days of cell injection in mice. (C) Tumor weight was determined in resected tumors after 35 days. (D) The expression levels of circFIG 4, miR-493-5p, and E2F3 mRNA were assessed by qRT-PCR. (E) The protein level of E2F3 was tested via western blot. (F) Immunohistochemistry assay was conducted for the expression of ki-67 in EC tissues. The total score of ki-67 immunoreactivity was significantly lower in the sh-circFIG 4 group compared to that in the sh-NC group. $^{**}p < 0.01$, $^{***}p < 0.001$

cells, whereas co-transfection of sh-circFIG 4 and in-miR-493-5p reversed the effect (Figure 7A,B). Furthermore, E2F3 expression was negatively correlated with miR-493-5p level ($p < 0.0001$, $r = -0.6133$) and positively correlated with circFIG 4 expression ($p < 0.0001$, $r = 0.6674$) in EC tissues (Figure 7C,D). Taken together, circFIG 4 positively regulated E2F3 expression by targeting miR-497-5p.

Knockdown of circFIG 4 blocked the tumorigenesis of EC in vivo

To estimate the effect of circFIG 4 on tumor growth in vivo, xenograft mice models were established by injecting KYSE-150 cells transfected with lentivirus-mediated sh-NC or sh-circFIG 4 into nude mice. As shown in Figure 8A–C, tumor volume and weight were distinctly hampered in the sh-circFIG 4 group compared to the sh-NC group. Moreover, levels of circFIG 4, E2F3 mRNA, and E2F3 protein were remarkably reduced and miR-493-5p expression was overtly raised in tumor tissues derived from sh-circFIG 4-transfecting cells (Figure 8D,E). Immunohistochemistry (IHC) assay showed reduced expression ki-67 in EC tissues, and the total score of ki-67 immunoreactivity was significantly lower in the tumor tissues of the sh-circFIG 4 group versus that in the sh-NC group (Figure 8F). Thus, it was deduced that circFIG 4 depletion hindered tumor growth in vivo through the dependence of the miR-493-5p/E2F3 axis.

DISCUSSION

Numerous studies have demonstrated that circRNAs are concerned with the biologic processes of cancer by regulating many pathways.[19,20] Studies have also demonstrated that the imbalance of circRNA levels exerts essential function in regulating EC development.[8,21] However, the effects of circFIG 4 on EC development have not been investigated. Here, we attested that circFIG 4 level was enhanced in EC. Functionally and mechanically, circFIG 4 silence suppressed the aggressive behaviors of EC cells through affecting the miR-493-5p/E2F3 axis. A recent report showed that circFIG 4 was overtly downregulated in lung adenocarcinoma patients.[22] Moreover, circFIG 4 was identified to be abundantly expressed in EC tissues.[10] Here, we also confirmed that circFIG 4 was abundantly expressed in EC tissues and cells. Further function analysis revealed that circFIG 4 knockdown curbed the proliferative and transferable capacities and accelerated the apoptotic ability of EC cells. Moreover, circFIG 4 silence also restrained the tumorigenesis of EC in vivo. These results illustrate that circFIG 4 exerts a carcinogenic effect on EC progression.

circRNAs have been certified to take part in modulating a battery of intracellular courses through serving as the sponges of miRNAs.[23] Herein, it was identified that circFIG 4 could function as a molecular decoy for miR-493-5p. Furthermore, miR-493-5p could function as an antitumor factor in different types of malignancies, including hepatocellular carcinoma,[24] melanoma,[25] and neuroblastoma.[26] However, study concerning the specific function of miR-493-5p in EC is still limited. According to recent research, the enrichment of miR-493 was distinctly reduced in EC, and miR-493 overexpression could attenuate the propagation and transferability of EC cells.[17] In the present report, we found that the miR-493-5p level was markedly decreased in EC. Meanwhile, miR-493-5p introduction also restricted the malignant properties of EC cells. Furthermore, miR-493-5p silence alleviated the inhibiting effect of circFIG 4 deficiency on EC cell progression, indicating that circFIG 4 regulated EC cell malignant behaviors by competitively binding to miR-493-5p.

Furthermore, E2F3 was shown to be targeted by miR-493-5p. The interaction of miRNAs and E2F3 in regulating human cancers was proposed, and E2F3 was verified to exert a carcinogenic role in diverse tumors.[27] For instance, lncRNA SNHG22 could accelerate the development of colorectal cancer by sponging miR-128-3p and upregulating E2F3 expression,[28] and miR-573 suppressed cell progression in pancreatic cancer through regulating E2F3.[29] Likewise, E2F3 had elevated levels in esophageal squamous cell carcinoma (ESCC), and circ_0087378 deficiency blocked ESCC cell progression by enhancing E2F3 expression.[30] Here, we discovered that the abundance of E2F3 was raised in EC tissues and cells. Moreover, E2F3 introduction relieved the suppressive influences of miR-493-5p overexpression on EC cell development. In addition, the expression of E2F3 was inhibited by circFIG 4 knockdown, while the effect was abrogated by miR-493-5p inhibition. These data hinted that circFIG 4 knockdown could impede the malignant phenotypes of EC through affecting the miR-493-5p/E2F3 pathway.

In conclusion, our findings revealed that circFIG 4 expression was elevated in EC tissues and cells. In addition, circFIG 4 could facilitate the malignancy of EC via the miR-493-5p/E2F3 axis. The newfound modulatory axis might provide a potential remedial strategy for EC therapy.

ACKNOWLEDGMENTS

None.

CONFLICT OF INTEREST

The authors declare that they have no conflicts of interest.

ORCID

Zhen Huang https://orcid.org/0000-0003-2824-0244
Xin Zhao https://orcid.org/0000-0002-5598-2158

REFERENCES

1. Alsop BR, Sharma P. Esophageal cancer. Gastroenterol Clin North Am. 2016;45:399–412.
2. Kato H, Nakajima M. Treatments for esophageal cancer: a review. Gen Thorac Cardiovasc Surg. 2013;61:330–5.
3. Lan T, Xue X, Dunmall LC, et al. Patient-derived xenograft: a developing tool for screening biomarkers and potential therapeutic targets for human esophageal cancers. Aging (Albany NY). 2021;13:12273–93.

4. Qian L, Yu S, Chen Z, et al. The emerging role of circRNAs and their clinical significance in human cancers. Biochim Biophys Acta Rev Cancer. 2018;1870:247–60.
5. Hansen TB, Jensen TI, Clausen BH, et al. Natural RNA circles function as efficient microRNA sponges. Nature. 2013;495:384–8.
6. Kristensen LS, Hansen TB, Veno MT, et al. Circular RNAs in cancer: opportunities and challenges in the field. Oncogene. 2018;37:555–65.
7. Ma Z, Shuai Y, Gao X, et al. Circular RNAs in the tumour microenvironment. Mol Cancer. 2020;19:8.
8. Sun Y, Qiu L, Chen J, et al. Construction of circRNA-associated ceRNA network reveals novel biomarkers for esophageal cancer. Comput Math Methods Med. 2020;2020:7958362.
9. Zhang LW, Wang B, Yang JX, et al. Circ-PRMT5 stimulates migration in esophageal cancer by binding miR-203. Eur Rev Med Pharmacol Sci. 2020;24:9965–72.
10. Shi P, Sun J, He B, et al. Profiles of differentially expressed circRNAs in esophageal and breast cancer. Cancer Manag Res. 2018;10:2207–21.
11. Shi Y, Fang N, Li Y, et al. Circular RNA LPAR3 sponges microRNA-198 to facilitate esophageal cancer migration, invasion, and metastasis. Cancer Sci. 2020;111:2824–36.
12. Mendell JT, Olson EN. MicroRNAs in stress signaling and human disease. Cell. 2012;148:1172–87.
13. Peng Y, Croce CM. The role of MicroRNAs in human cancer. Signal Transduct Target Ther. 2016;1:15004.
14. O'Brien J, Hayder H, Zayed Y, et al. Overview of microRNA biogenesis, mechanisms of actions, and circulation. Front Endocrinol (Lausanne). 2018;9:402.
15. Gu S, Jin L, Zhang F, et al. Biological basis for restriction of microRNA targets to the 3' untranslated region in mammalian mRNAs. Nat Struct Mol Biol. 2009;16:144–50.
16. Sakai NS, Samia-Aly E, Barbera M, et al. A review of the current understanding and clinical utility of miRNAs in esophageal cancer. Semin Cancer Biol. 2013;23:512–21.
17. Bian W, Li Y, Zhu H, et al. miR-493 by regulating of c-Jun targets Wnt5a/PD-L1-inducing esophageal cancer cell development. Thorac Cancer. 2021;12:1579–88.
18. Striefler JK, Riess H, Lohneis P, et al. Mucin-1 protein is a prognostic marker for pancreatic ductal adenocarcinoma: results from the CONKO-001 study. Front Oncol. 2021;11:670396.
19. Shang Q, Yang Z, Jia R, et al. The novel roles of circRNAs in human cancer. Mol Cancer. 2019;18:6.
20. Zhu Y, Gu J, Li Y, et al. MiR-17-5p enhances pancreatic cancer proliferation by altering cell cycle profiles via disruption of RBL2/E2F4-repressing complexes. Cancer Lett. 2018;412:59–68.
21. Niu C, Zhao L, Guo X, et al. Diagnostic accuracy of circRNAs in esophageal cancer: a meta-analysis. Dis Markers. 2019;2019:9673129.
22. Chen Z, Wei J, Li M, et al. A circular RNAs dataset landscape reveals potential signatures for the detection and prognosis of early-stage lung adenocarcinoma. BMC Cancer. 2021;21:781.
23. Panda AC. Circular RNAs act as miRNA sponges. Adv Exp Med Biol. 2018;1087:67–79.
24. Yang G, Xu Q, Wan Y, et al. Circ-CSPP1 knockdown suppresses hepatocellular carcinoma progression through miR-493-5p releasing-mediated HMGB1 downregulation. Cell Signal. 2021;86:110065.
25. Bai M, Wu ZZ, Huang YL, et al. STAT3 activates the transcription of lncRNA NR2F1-AS1 to promote the progression of melanoma via regulating the miR-493-5p/GOLM1 axis. J Gene Med. 2021;23:e3338.
26. Liu L, Zhao H, He HH, et al. Long non-coding RNA NR2F1-AS1 promoted neuroblastoma progression through miR-493-5p/TRIM2 axis. Eur Rev Med Pharmacol Sci. 2020;24:12748–56.
27. Gao Y, Feng B, Lu L, et al. MiRNAs and E2F3: a complex network of reciprocal regulations in human cancers. Oncotarget. 2017;8:60624–39.
28. Yao J, Wang C, Dong X, et al. lncRNA SNHG22 sponges miR1283p to promote the progression of colorectal cancer by upregulating E2F3. Int J Oncol. 2021;59:71.
29. Pengcheng Z, Peng G, Haowen F, et al. MiR-573 suppresses cell proliferation, migration and invasion via regulation of E2F3 in pancreatic cancer. J Cancer. 2021;12:3033–44.
30. Wang J, Wang Q, Gong Y, et al. Knockdown of circRNA circ_0087378 represses the tumorigenesis and progression of esophageal squamous cell carcinoma through modulating the miR-140-3p/E2F3 Axis. Front Oncol. 2020;10:607231.

SUPPORTING INFORMATION

Additional supporting information may be found in the online version of the article at the publisher's website.

How to cite this article: Huang Z, Wang C, Zhao X. circFIG 4 drives the carcinogenesis and metastasis of esophagus cancer via the miR-493-5p/E2F3 axis. Thorac Cancer. 2022;13:783–94. https://doi.org/10.1111/1759-7714.14321